

WHERE IS THE MEAN-FIELD TRANSITION TEMPERATURE OF UNDERDOPED SUPERCONDUCTING CUPRATES HIDING?

L. MIU

National Institute of Materials Physics, 77125 Bucharest-Magurele, P. O. Box MG-7, Romania

(Received March 20, 2008)

Abstract. Recent models for the occurrence of high-temperature superconductivity predict that the superconducting transition of underdoped cuprates is determined by the phase fluctuations of the order parameter, while the modulus of the wave function remains finite up to the pseudogap temperature T^* . Here we show that the mean-field transition temperature cannot be identified with T^* .

Key words: High-temperature superconductivity, cuprates, pseudogap, mean-field transition temperature, BKT transition.

1. INTRODUCTION

Exhibiting superconductivity at surprisingly high temperatures [1], the cuprates became the best studied materials outside the semiconductor family. There are hundreds of such high-temperature superconductors (HTS), but they all share a layered structure made up of one or more Cu-O planes. It is now generally accepted that the parent compound is a Mott insulator, which describes the situation where the material should be metallic according to the band theory, but is insulating due to the strong electron-electron repulsion. It also results that this Mott insulator should be an antiferromagnetic insulator, since when neighboring spins are oppositely aligned one can gain a significant energy (the exchange energy) by virtual hopping. The Cu-O planes of the parent compound (La_2CuO_4 , for example) can be hole-doped by substituting some of the trivalent La by divalent Sr. The antiferromagnetism is gradually suppressed by doping, and superconductivity appears for a certain doping interval. The proximity between the two phases suggests that the pairing may involve magnetic excitations, as well [2].

In conventional low- T_c superconductors, developing from the metallic state, the superconducting–normal transition implies the vanishing of the macroscopic wave function, and the ratio between the superconducting energy gap and T_c is constant. For HTS known at present, growing out from insulators, a (pseudo)gap opens

below T^* (the pseudogap temperature) [3], which increases with decreasing doping, and may be of magnetic origin. At low doping levels T^* is much higher than T_c , since the latter exhibits an opposite doping dependence. To connect the pseudogap opening at $T \sim T^*$ and the resistive transition at $T_c \ll T^*$, a phase fluctuation scenario was developed for the superconducting transition of underdoped cuprates [2, 4, 5]. According to this scenario, owing to a reduced superfluid density (low phase stiffness) in underdoped cuprates, the resistive transition at T_c is caused by the proliferation of vortices, which destroys the long-range phase coherence at T_c , whereas the modulus of the wave function (the superfluid density) remains finite up to much higher T values, of the order of T^* . This approach was further stimulated by the observation of a strong Nernst signal at T well above T_c , which was attributed to vortices [6], and the new concept of “Abrikosov vortices in the normal state” of underdoped HTS was born (although some other sources for the Nernst signal have been proposed). If the mean-field transition temperature T_{c0} can be related to T^* is still an open question, and our discussion below is based on the analysis of the zero-magnetic-field resistive transition and the current–voltage (I – V) characteristics of underdoped HTS.

2. RESISTIVE TRANSITION OF UNDERDOPED HTS

Optimally doped HTS exhibit an almost linear T variation of the in-plane electrical resistivity ρ for T above T_c . By contrast, the underdoped specimens show an upward curvature in $\rho(T)$ for T above T_c , as can be seen in Fig. 1, for an underdoped

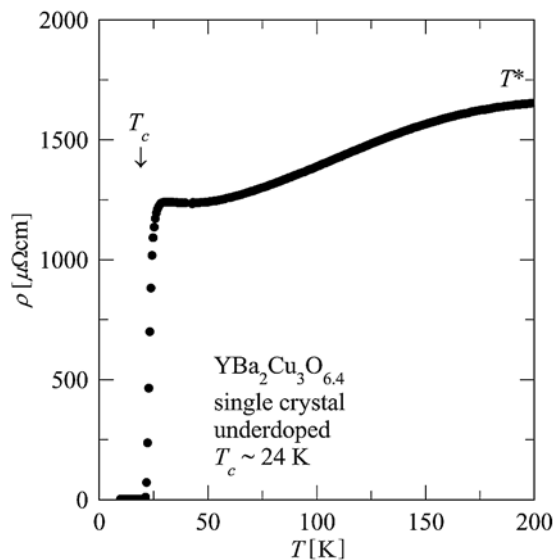


Fig. 1 – Zero-field resistive transition $\rho(T)$ of a (heavily underdoped) YBa₂Cu₃O_{6.4} single crystal for a low transport current density. Note the decrease of ρ with decreasing T appearing below T^* , and the large difference between T^* and T_c .

YBa₂Cu₃O_{~6.4} single crystal. It is tempting to identify the T value below which ρ starts decreasing with decreasing T with the pseudogap temperature T^* , because these are close each other. As noted above, in the vortex fluctuation (or preformed pair) scenario it is considered that the finite ρ in the limit of small transport currents in HTS occurs at T_c due to the phase fluctuations of the order parameter. In zero external magnetic field the phase fluctuations manifest themselves through the occurrence of vortex (V) – antivortex (A) pairs, and the V-A pair dissociation will drive the transition.

As argued in Ref. [4], the theory of T_c of these materials should be then that of the Berezinskii-Kosterlitz-Thouless (BKT) transition temperature T_{KT} at the superconducting Cu-O layer level. Above $T_c \equiv T_{KT}$, a state of paired charge carriers with short-range and short-time phase correlations was proposed, to account for the anomalous properties observed in the pseudogap region (between T_c and T^*). On the other hand, the mean-field critical temperature T_{c0} (where the superfluid density n_s should vanish) and T_{KT} are intimately related in the case of a BKT transition [7]. In this situation, the analysis of the vortex-antivortex unbinding process (supplying both T_{KT} and T_{c0}) would be a good test for the scenario proposed in Refs. [2, 4–6].

3. VORTEX-ANTIVORTEX UNBINDING IN HTS

The vortex (V) – antivortex (A) unbinding process is briefly reviewed below. Similar to He⁴ films and 2D Josephson junctions, the superconducting thin films undergo a BKT transition from the superfluid to the dissipative state [7–9]. This transition is driven by thermally created V-A pairs, which start to unbind at T_{KT} . For a superconducting thin film, the energy of a 2D V-A pair of separation r is [8] $E(r) \approx 2E_c + E_{1f} \ln(r/\xi)$, where E_c is the core energy, ξ is the (in-plane) coherence length, and E_{1f} is the V-A coupling constant. The latter is related to the penetration depth λ and to the dielectric constant ε (incorporating the screening of the interaction due to the presence of other pairs with smaller separations): $E_{1f} = dk_B \Phi_0^2 / 2\pi\varepsilon\mu_0\lambda^2$, where d is the film thickness. Below T_{KT} , $\varepsilon(T) \approx 1$, and one has $E_{1f} \propto 1/\lambda^2 \propto n_s$. Due to the contribution of entropy to the free energy, excitation of free 2D vortices becomes thermodynamically favorable above $T_{KT} = E_{1f}(T_{KT})/4k_B$ [9], where the vortex pairs thermally unbind at the certain scale, which decreases with increasing T . While for superconducting thin films the logarithmic interaction is cut off at the scale $\sim 2\lambda^2/d$ [9], for layered superconductors without interlayer Josephson coupling the in-plane logarithmic interaction is present at large intervortex separations, as well, due to the field redistribution generated by the screening produced by the other layers. Neglecting the magnetic

coupling between vortices located in different layers, these systems are expected to exhibit BKT-type behavior.

Due to their large intrinsic anisotropy, the underdoped HTS can be regarded as systems of weakly coupled superconducting Cu-O layers. For V-A separations larger than the Josephson length γs , where γ is the anisotropy parameter and s is the interlayer spacing, the energy of a quasi-2D V-A pair in the presence of a transport current density J is $E(r, J) \approx 2E_c + E_1 \ln(r/\xi) + E_2(r/\xi) - s\Phi_0 J r$, where the in-plane coupling constant $E_1 = s k_B \Phi_0^2 / 2\pi\epsilon\mu_0 \lambda^2$. The positive term linear in r appears due to the interlayer Josephson coupling [10, 11] ($E_2 = E_1 \xi / \gamma s$), giving rise to a finite zero-field critical-current density $J_c = E_2 / s\Phi_0 \xi$. $E(r)$ has a maximum for $r_m = E_1 / [s\Phi_0(J - J_c)]$, and the current induced pair dissociation rate Γ_+ can be estimated as an escape rate over the barrier $\Delta E = E(r_m, J) - 2E_c$, *i.e.*, $\Gamma_+ \propto \exp(-\Delta E / k_B T) \propto J^{E_1 / k_B T}$. In the “free-drift” approach, it is considered that the voltage V results from the flow of free vortices, and the current-voltage (I - V) characteristic takes the form $V \propto I(I - I_c)^{E_1 / 2k_B T}$, where I_c is the critical current. However, it was shown that for a relatively large vortex density the main contribution to $V(I)$ appears from the motion of temporarily bound vortices on a distance $\sim r_m$. Both the “pair-stretching” [12] and “partner transfer” [13] models lead for the quasi-2D regime to

$$V \propto (I - I_c)^a, \quad (1)$$

and the T dependence of the I - V curve exponent a is given by

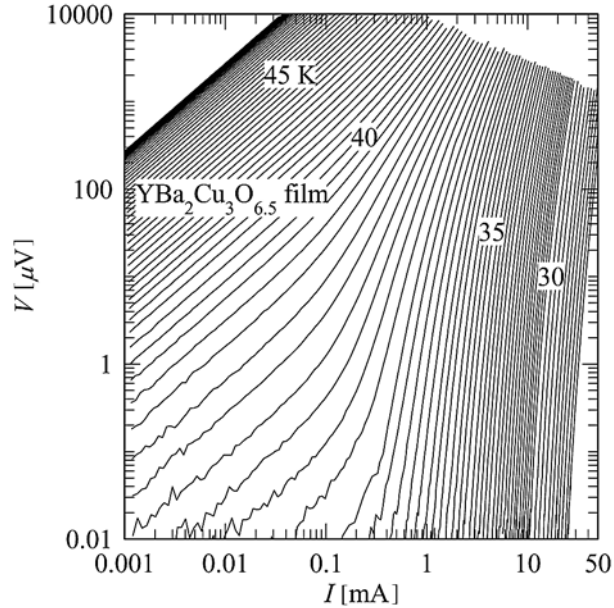
$$a(T) = -1 + E_1 / k_B T, \quad (2)$$

in agreement with dynamical simulations of the classical XY model and recent experimental results obtained for highly anisotropic $\text{Bi}_2\text{Sr}_2\text{CaCu}_2\text{O}_{8+\delta}$ films [14, 15]. All the above approaches fulfill the condition $a(T_{KT}) = 3$ for a BKT transition. With Eq. (2), one can determine the mean-field critical temperature T_{c0} by extrapolating the $a(T)$ variation determined for $T < T_{KT}$ to $a(T_{c0}) = -1$ [$E_1(T_{c0}) = 0$]. It is worth noting that a significant pinning will introduce another (positive) term linear in r in the V-A pair energy relation used above, which leads to an increase the actual critical current, but has little effect on the I - V curve exponent.

We measured the I - V curves of underdoped $\text{YBa}_2\text{Cu}_3\text{O}_x$ films ($x \sim 6.5, 6.55,$ and 6.65) in a magnetically shielded environment [16]. The films ($d \sim 250$ nm) were prepared by an *in-situ* sputtering method on (100) oriented SrTiO_3 substrates, and different doping levels were attained by annealing the as-grown films for different time intervals at 550°C in a 1 mbar oxygen atmosphere.

The evolution of the I - V curves with T is illustrated in Fig. 2, for the sample $\text{YBa}_2\text{Cu}_3\text{O}_{\sim 6.5}$. The other underdoped films show a similar behavior. At low T , the I - V curves exhibit a downward curvature in the log-log plot, reflecting the occurrence of a finite I_c due to the interlayer Josephson coupling.

Fig. 2 – In-plane zero-magnetic-field current-voltage (I - V) characteristics of the underdoped $\text{YBa}_2\text{Cu}_3\text{O}_{\sim 6.5}$ film, for T between 25 K and 50 K. The step in T was 0.25 K above 30 K and 0.5 K between 25 and 30 K.



The exponent a was obtained from the fit of the I - V curves with the $V(I)$ relation for the quasi-2D regime Eq. (1), as illustrated in the inset to Fig. 3. In the (V, I) window of our measurements, the I - V curves can be fitted with Eq. (1) up to $T \sim 32$ K [16].

The resulting $a(T)$ variation is shown in the main panel of Fig. 3. The determined $a(T)$ follows Eq. (2) with a linear T decrease of $E_1(T) \propto 1/\lambda^2$, as reported for underdoped cuprates. The value $a = 3$ indicates a T_{KT} value at the Cu-O bi-layer level of ≈ 33 K, whereas the extrapolation of the $a(T)$ variation leads to a mean-field critical temperature $T_{c0} \approx 47$ K. The fit in the main panel of Fig. 2 gives $\lambda(0) \approx 330$ nm, in excellent agreement with λ determined from complex conductivity measurements.

In connection to the above location of T_{KT} and T_{c0} , a question which may arise is if the $a(T)$ dependence plotted in the main panel of Fig. 3 represents the T variation of the bare superfluid density. This is not obvious in the vortex fluctuation scenario, where the proposed state with short-time phase correlations at high T can affect the T_{KT} and T_{c0} values determined in a dc experiment. In this context, it has to be emphasized that the zero-field I - V curves from Fig. 2 describe

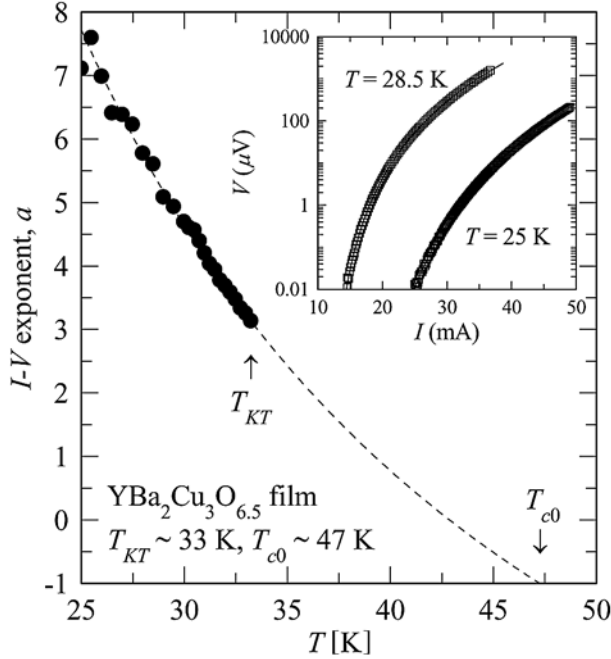


Fig. 3 – T variation of the quasi-2D I - V exponent a for the underdoped $\text{YBa}_2\text{Cu}_3\text{O}_{6.5}$ film, determined by the fit of the I - V curves with Eq. (1), as shown in the inset. The dashed line in the main panel represents the one parameter fit of the $a(T)$ data with Eq. (2). The results are $T_{KT} \approx 33$ K, and $T_{c0} \approx 47$ K.

a continuous process of vortex creation and recombination. The model in which the voltage V is generated by temporarily bound vortices allows an estimation of the life-time of a V-A pair. It can easily be shown that with an “effective magnetic field” created by thermally excited vortices of the order of 10 G the life-time of the vortex pairs probed at $T = 30$ K and $V \sim 100$ μV , for example, is the time interval in which a vortex moves over the distance $r_m \sim 1$ μm , and is of the order of 10^{-8} s. Since the dynamics reported in Ref. [17] reveals a rapid increase of the “phase correlation time” on approaching T_{KT} from above, one can conclude that $a(T)$ from the main panel of Fig. 2 represents the T variation of the bare superfluid density.

3. THE 2D COULOMB GAS ANALYSIS OF $\rho(T)$

We need, however, a confirmation of the T_{KT} and T_{c0} values determined from the analysis of the $a(T)$ variation. Fortunately, in the case of highly anisotropic HTS, this can be done by using the 2D behavior appearing at high T , where Monte Carlo simulations [18] and renormalization group analyses [19] reveal the decoupling of the superconducting layers due to the proliferation of zero-field vortex fluctuations.

Thus, it becomes appropriate to represent the T dependence of the electrical resistivity $\rho(T)$ in the framework of the Ginzburg-Landau 2D Coulomb gas model

[20], which predicts that certain measurable quantities only depend on the dimensionless variable $X = (T/T_{KT})(T_{c0} - T_{KT})/(T_{c0} - T)$. Since $T/X \propto T_{c0} - T$, one can determine T_{c0} by linear extrapolation, whereas T_{KT} results from the condition $X(T_{KT}) = 1$, if the variable $X(T)$ is extracted independently. With $\rho(T)$ following the universal 2D scaling curve [20], $X(T)$ is obtained from the experimental $\rho(T)$ data.

The plot T/X versus T for the resistive transitions of the $\text{YBa}_2\text{Cu}_3\text{O}_{\sim 6.4}$ single crystal (Fig. 1) and $\text{YBa}_2\text{Cu}_3\text{O}_{\sim 6.5}$ film measured with a low transport current density is shown in Fig. 4. The linear dependence (decoupled $(\text{CuO}_2)_2$ layers) appears at high T . The extrapolation in Fig. 4 and the definition of the variable X lead to $T_{c0} \approx 25$ K and $T_{KT} \approx 18$ K for $\text{YBa}_2\text{Cu}_3\text{O}_{\sim 6.4}$. The values for the $\text{YBa}_2\text{Cu}_3\text{O}_{\sim 6.5}$ film are practically identical to those supplied by the analysis of the $a(T)$ variation. It is worth noting that the high- T 2D behavior is cut-off at low T , where the interlayer Josephson coupling sets in [16].

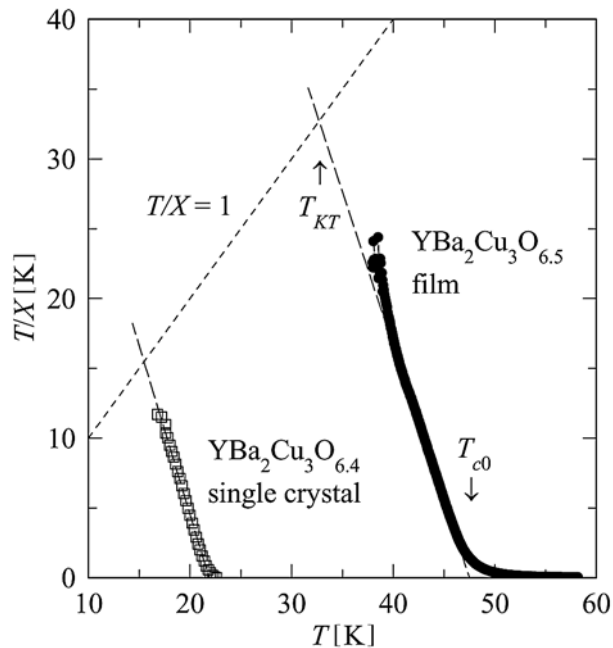


Fig. 4 – The zero-field resistive transition of $\text{YBa}_2\text{Cu}_3\text{O}_{\sim 6.4}$ single crystal and of $\text{YBa}_2\text{Cu}_3\text{O}_{\sim 6.5}$ film analyzed in the framework of the 2D Coulomb gas model (see text).

Finally, a very schematic doping diagram for the $\text{YBa}_2\text{Cu}_3\text{O}_x$ family is illustrated in Fig. 5, where we included the T_{c0} and T_{KT} values determined by us for underdoped samples. Both T_{c0} and T_{KT} increase with doping, which is opposite to $T^*(x)$. The T dependence of the in-plane electrical resistivity $\rho(T)$ of the $\text{YBa}_2\text{Cu}_3\text{O}_{\sim 6.5}$ film for a measuring current of $50 \mu\text{A}$ is shown in the inset to Fig. 5, where the T_{KT} and T_{c0} determined in Fig. 4 are indicated by arrows. Note that T_{KT} lies

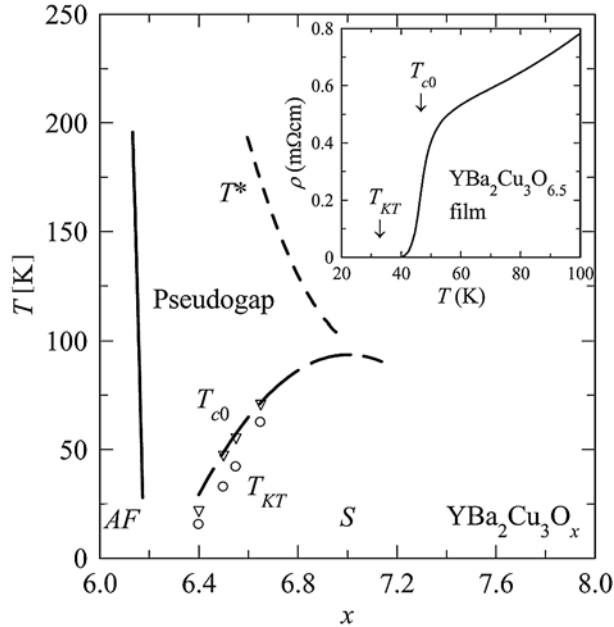


Fig. 5 – Schematic doping diagram for $\text{YBa}_2\text{Cu}_3\text{O}_x$, in which we added the mean-field transition temperature T_{c0} and the BKT transition temperature T_{KT} values determined by us for underdoped specimens. AF and S represent the antiferromagnetic and superconducting phases. The inset shows $\rho(T)$ for the $\text{YBa}_2\text{Cu}_3\text{O}_{6.5}$ film, where T_{KT} and T_{c0} determined in Fig. 4 are indicated by arrows.

below the drop in $\rho(T)$, whereas T_{c0} is located very close to the inflection point in $\rho(T)$, *i.e.*, $T_{c0} = T_c$.

In conclusion, we investigated the T variation of the zero-field in-plane I - V curve exponent of high-quality oxygen deficient $\text{YBa}_2\text{Cu}_3\text{O}_x$ films in the framework of the quasi-2D vortex-antivortex unbinding model, where the I - V exponent is directly related to the superfluid density. The extracted T dependence of this exponent indicates that the mean-field transition temperature T_{c0} remains in the domain of the resistivity drop, which is confirmed by the analysis of the resistive transition of several underdoped $\text{YBa}_2\text{Cu}_3\text{O}_x$ films and single crystals in the framework of the Ginzburg-Landau 2D Coulomb gas model.

We suggest that T_{c0} cannot be identified with the pseudogap temperature T^* , since T_{c0} and T^* involve different energy scales and have a different doping dependence. Our results cast some doubt on the presence of “Abrikosov vortices above T_c ” in underdoped HTS.

This work was supported by the Ministry of Education and Research at NIMP Bucharest, and by the Alexander von Humboldt Foundation at the University of Mainz.

REFERENCES

1. J. G. Bednorz, K. A. Mueller, *Possible high- T_c superconductivity in the La-Ba-Cu-O system*, Z. Phys. B, **64**, 189–193 (1986).

2. P. W. Anderson, *Physics of the Resonating Valence Bond (Pseudogap) state of the doped Mott insulator: Spin-charge locking*, Phys. Rev. Lett., **96**, 017001 (2006).
3. Ch. Renner, B. Revaz, J. Y. Genoud, K. Kadowaki, Ø. Fischer, *Pseudogap precursor of the superconducting gap in under- and overdoped $\text{Bi}_2\text{Sr}_2\text{CaCu}_2\text{O}_{8+\delta}$* , Phys. Rev. Lett., **80**, 149–152 (1998).
4. P. A. Lee, *Doping a Mott insulator: Physics of high-temperature superconductivity*, Rev. Mod. Phys., **78**, 17–87 (2006).
5. C. Meingast, V. Pasler, P. Nagel, A. Rykov, S. Tajima, P. Olsson, *Phase fluctuations and the pseudogap in $\text{YBa}_2\text{Cu}_3\text{O}_x$* , Phys. Rev. Lett., **86**, 1606–1609 (2001).
6. Y. Wang, L. Li, N. P. Ong, *Nernst effect in high- T_c superconductors*, Phys. Rev. B, **73**, 024510 (2006).
7. J. M. Kosterlitz, D. J. Thouless, *Long range order and metastability in two dimensional solids and superfluids*, J. Phys. C, **5**, L124–L126 (1972).
8. A. M. Kadin, K. Epstein, A. M. Goldman, *Renormalization of the Kosterlitz-Thouless transition in a two-dimensional superconductor*, Phys. Rev. B, **27**, 6691–6702 (1983).
9. G. Blatter, M. V. Feigel'man, V. B. Geshkenbein, A. I. Larkin, V. M. Vinokur, *Vortices in high-temperature superconductors*, Rev. Mod. Phys., **66**, 1125–1388 (1994).
10. H. J. Jensen, P. Minnhagen, *Two-dimensional fluctuations in the nonlinear current-voltage characteristics for high-temperature superconductors*, Phys. Rev. Lett., **66**, 1630–1633 (1991).
11. L. Miu, P. Wagner, U. Frey, A. Hadish, Dana Miu, H. Adrian, *Vortex unbinding and layer decoupling in epitaxial $\text{Bi}_2\text{Sr}_2\text{Ca}_2\text{Cu}_3\text{O}_{10+\delta}$ thin films*, Phys. Rev. B, **52**, 4553–4558 (1995).
12. P. Minnhagen, O. Westman, A. Jonsson, P. Olsson, *New exponent for the nonlinear IV characteristics of a two dimensional superconductor*, Phys. Rev. Lett., **74**, 3672–3675 (1995).
13. D. Bormann, *Charge transport in the dense two-dimensional Coulomb gas*, Phys. Rev. Lett., **78**, 4324–4327 (1997).
14. L. Miu, G. Jakob, P. Haibach, Th. Kluge, U. Frey, P. Voss-de Haan, H. Adrian, *Length-scale-dependent vortex-antivortex unbinding in epitaxial $\text{Bi}_2\text{Sr}_2\text{CaCu}_2\text{O}_{8+\delta}$ films*, Phys. Rev. B, **57**, 3144–3150 (1998).
15. L. Miu, D. Miu, G. Jakob, H. Adrian, *Determination of two-dimensional zero-magnetic-field I-V exponent in $\text{Bi}_2\text{Sr}_2\text{CaCu}_2\text{O}_{8+\delta}$* , Phys. Rev. B, **73**, 224526 (2006).
16. L. Miu, D. Miu, G. Jakob, H. Adrian, *Location of the mean-field critical temperature of underdoped $\text{YBa}_2\text{Cu}_3\text{O}_{7-\delta}$ films*, Phys. Rev. B, **75**, 214504 (2007).
17. J. Corson, R. Mallozzi, J. Orenstein, J. N. Eckstein, I. Bozovic, *Vanishing of phase coherence in underdoped $\text{Bi}_2\text{Sr}_2\text{CaCu}_2\text{O}_{8+\delta}$* , Nature, **398**, 221–223 (1999).
18. H. Weber, H. J. Jensen, *Crossover from three- to two-dimensional behavior of the vortex energies in layered XY models for high- T_c superconductors*, Phys. Rev. B, **44**, 454–457 (1991).
19. S. W. Pierson, *Length-scale dependent layer decoupling in layered systems*, Phys. Rev. Lett., **75**, 4674–4677 (1995).
20. P. Minnhagen, *The two-dimensional Coulomb gas, vortex unbinding, and superfluid-superconducting films*, Rev. Mod. Phys., **59**, 1001–1066 (1987).